

Papers published in *Hydrology and Earth System Sciences Discussions* are under open-access review for the journal *Hydrology and Earth System Sciences*

# Mapping rainfall erosivity at a regional scale: a comparison of interpolation methods in the Ebro Basin (NE Spain)

M. Angulo-Martínez<sup>1</sup>, M. López-Vicente<sup>1</sup>, S. M. Vicente-Serrano<sup>2</sup>, and S. Beguería<sup>1</sup>

<sup>1</sup>Department of Soil and Water, Aula Dei Experimental Station–CSIC. 1005 Avda. Montañana, 50080 Zaragoza, Spain

<sup>2</sup>Department of Geo-environmental Processes and Global Change, Pyrenean Institute of Ecology–CSIC. 1005 Avda. Montañana, 50080 Zaragoza, Spain

Received: 25 November 2008 – Accepted: 26 November 2008 – Published: 19 January 2009

Correspondence to: M. Angulo-Martínez (mangulo@eead.csic.es)

Published by Copernicus Publications on behalf of the European Geosciences Union.

**HESSD**

6, 417–453, 2009

## Mapping rainfall erosivity at a regional scale

M. Angulo-Martínez et al.

Title Page

Abstract

Introduction

Conclusions

References

Tables

Figures

◀

▶

◀

▶

Back

Close

Full Screen / Esc

Printer-friendly Version

Interactive Discussion



## Abstract

Rainfall erosivity is a major causal factor of soil erosion, and it is included in many prediction models. Maps of rainfall erosivity indices are required for assessing soil erosion at the regional scale. In this study a comparison is made between several techniques for mapping the rainfall erosivity indices: i) the RUSLE  $R$  factor and ii) the average  $EI_{30}$  index of the erosive events over the Ebro basin (NE Spain). A spatially dense precipitation data base with a high temporal resolution (15 min) has been used. Global, local and geostatistical interpolation techniques were employed to produce maps of the rainfall erosivity indices, as well as mixed methods (regression plus local interpolation). To determine the reliability of the maps several goodness-of-fit and error statistics were computed, using a cross-validation scheme. All methods represented correctly the spatial patterns of both erosivity indices, but the mixed approaches tended to be better overall considering the validation statistics. Additionally, they allowed identifying statistically significant relationships between rainfall erosivity and other geographical variables, as elevation and distance to the water bodies. All models had a relatively high uncertainty, caused by the high variability of rainfall erosivity indices both in time and space, what stresses the importance of using the longest data series available with a good spatial coverage.

## 1 Introduction

Soil erosion has become a major environmental threat due to the growth of the World's population, and is one of the main consequences of projected land use and climate change scenarios (Gobin et al., 2004). Studies on soil erosion started in the first decades of the 20th Century, and have increased in number and variety since then. Isolating the role of different natural and management factors on soil erosion has been one of the major research topics. The combination of those factors in the form of a parametric model allowed the development of tools such as the USLE (Wischmeier

**HESSD**

6, 417–453, 2009

### Mapping rainfall erosivity at a regional scale

M. Angulo-Martínez et al.

Title Page

Abstract

Introduction

Conclusions

References

Tables

Figures

◀

▶

◀

▶

Back

Close

Full Screen / Esc

Printer-friendly Version

Interactive Discussion



and Smith, 1978; Kinnell and Risse, 1998), which can be used for predicting the effect of different management strategies on soil erosion rates. The development of parametric models opened a new area of research, devoted to analyze the spatial variability of erosion causal factors. Maps showing the spatial distribution of natural and management related erosion factors are of great value in the early stages of land management plans, allowing identify preferential areas where action against soil erosion is more urgent or where the remediation effort will have highest revenue. With the advent of Geographic Information Systems (GIS), studies of this kind have become more and more frequent.

Among the natural factors affecting soil erosion, rainfall erosivity has a paramount importance. Precipitation is a major cause of soil erosion, given the extraordinary importance of soil detachment processes due to drop impact and runoff shear. Compared to other natural factors such as the relief or the soil characteristics, rainfall erosivity has very little or null possibility of modification by humans, so it represents a natural environmental constrain that limits and conditions land use and management. In the context of climate change, the effect of altered rainfall characteristics on soil erosion is one of the main concerns of soil conservation studies.

It is well known that a few, very intense rainfall events are responsible for the largest part of the soil erosion and sediment delivery (González-Hidalgo et al., 2007). Hence, the estimation of rainfall erosivity may contribute to a better prediction of soil erosion. Rainfall erosivity can be quantified by several erosivity indices which evaluate the relationship between drop size distribution and kinetic energy of a given storm. Numerous works have assessed the role of drop size distribution of both natural and simulated rainfall at the field plot scale on soil detachment. These measurements are difficult to perform, and because of that they are very rare both in space and time. In addition, natural rainfall properties measurements are scarce for comparisons with simulated rain (Dunkerley, 2008). This has motivated researchers to undertake studies relating more conventional rainfall characteristics such as the maximum intensity during a period of time to rainfall energy or directly to soil detachment rates. Examples of such

## Mapping rainfall erosivity at a regional scale

M. Angulo-Martínez et al.

Title Page

Abstract

Introduction

Conclusions

References

Tables

Figures

◀

▶

◀

▶

Back

Close

Full Screen / Esc

Printer-friendly Version

Interactive Discussion



indices of rainfall erosivity are the USLE  $R$  factor, or the  $E/_{30}$  index (Wischmeier, 1959; Wischmeier and Smith, 1978; Brown and Foster, 1987; Renard and Freimund, 1994; Renard et al., 1997), the modified Fournier index for Morocco (Arnoldus, 1977), the  $KE>25$  index for southern Africa (Hudson, 1971) and the  $A/m$  index for Nigeria (Lal, 1976).

Mapping rainfall erosivity at regional and basin scale is still an emerging research question. Such maps allow for a better comprehension of the processes with geographical imprint as well as the application of these methodologies to large spatial areas. They are also an important step for large-scale soil erosion assessments, soil conservation management of natural resources, agronomy and agrochemical exposure risk assessments (Winchell et al., 2008). Early examples are the rainfall erosivity maps for the whole USA in the form of *isoerodent* maps or maps of the RUSLE  $R$  factor (Renard and Freimund, 1994). Other researchers have used regression techniques to elaborate spatially continuous maps of rainfall erosivity on the basis of other available data such as daily and monthly records of rainfall depth (ICONA, 1988).

With the advent of GIS packages and the generalization of spatial interpolation techniques, maps of environmental parameters such as those relevant for soil erosion have become frequent. For example, several authors have used GIS techniques to map the factors of the RUSLE equation by means of interpolation methods (Shi, 2004; Lim, 2005; Mutua, 2006; López-Vicente et al., 2008). There are a number of statistical methods available, such as regression models; local interpolators such as the inverse distance weighted (IDW) or thin-plate splines, or geostatistical techniques such as kriging (Burrough and McDonnell, 1998). Recent studies, mostly in the field of Climatology (e.g., Ninyerola and Pons, 2000; Vicente-Serrano et al., 2003; Beguería and Vicente-Serrano, 2006), highlighted the interest of finding the method with the best adjustment to the observed data.

There are few studies comparing between interpolation techniques for rainfall erosivity indices. Millward (1999) calculated the  $E/_{30}$  index at the monthly scale and the  $R$  factor with geostatistics and IDW techniques for the Algarve region (Southern Por-

## Mapping rainfall erosivity at a regional scale

M. Angulo-Martínez et al.

Title Page

Abstract

Introduction

Conclusions

References

Tables

Figures

◀

▶

◀

▶

Back

Close

Full Screen / Esc

Printer-friendly Version

Interactive Discussion



tugal). Hoyos (2005) observed that a local polynomial algorithm gave lower mean prediction errors than the IDW in the Colombian Andes. Goovaerts (1999) discussed the relation between rainfall erosivity and elevation in the comparison of three different geostatistical methods. None of these works provided a comprehensive comparison of mapping methods at the regional scale.

This work aims at comparing different interpolation methods to map the average  $EI_{30}$  index of the erosive events and the RUSLE  $R$  factor in a large and climatologically complex area: the Ebro basin, in north-eastern Spain. Results of rainfall erosivity cartography can be used as a reference for soil protection practices and discussion of the different interpolation methods will be of interest to enhance regional and basin cartography.

## 2 Materials and methods

### 2.1 Study area

The study area covers the north-east of Spain (Fig. 1). It corresponds to the Ebro Basin, which represents an area of about 85 000 km<sup>2</sup>. The Ebro valley is an inner depression surrounded by high mountain ranges. It is limited to the North by the Cantabrian Range and the Pyrenees, with maximum elevations above 3000 m a.s.l. The Iberian range closes the Ebro valley to the South, with maximum elevations in the range of the 2000–2300 m. To the East, parallel to the Mediterranean coast, the Catalan Coastal Range closes the Ebro valley, with maximum elevations between 1000 and 1200 m a.s.l.

The climate is influenced by the Cantabric and Mediterranean Seas and the effect of the relief on precipitation and temperature. The border mountain ranges isolate the central valley blocking the maritime influence, resulting in a continental climate which experiments aridity conditions (Cuadrat, 1991; Lana and Burgueño, 1998; Creus 2001; Vicente-Serrano, 2005). A climatic gradient in the NW-SE direction is remarkable,

## Mapping rainfall erosivity at a regional scale

M. Angulo-Martínez et al.

Title Page

Abstract

Introduction

Conclusions

References

Tables

Figures

◀

▶

◀

▶

Back

Close

Full Screen / Esc

Printer-friendly Version

Interactive Discussion



determined by the strong Atlantic influences in the north and north-west of the area during large part of the year and the Mediterranean influence to the east. Mountain ranges add complexity to the climate of the region. The Pyrenees extend the Atlantic influence to the east by increasing precipitation, whereas the Cantabrian Range, which runs parallel to the Atlantic coastland in the NW, is a barrier to the humid flows and has a noticeable climate contrast between the north (humid) and the south (dry) slopes.

The precipitation regime shows strong seasonality (Garrido and García, 1992), which involves not only the amount of precipitation but also its physical cause (frontal or convective). Precipitation in the inland areas is characterised by alternating wet and dry periods as a consequence of the seasonal displacement of the polar front and its associated pressure systems. Inter-annual variability of precipitation can be very high, and drought years can be followed by torrential rain events which last for many days (Martín-Vide, 1994).

Close to the Mediterranean Sea the precipitation amount also increases as a consequence of the maritime influence. Nevertheless, the precipitation frequency, intensity and seasonality are very different compared to the areas in the North, where precipitation is frequent but rarely very intense, with the exception of mountainous areas (García-Ruiz et al., 2000). The most extreme precipitation events are recorded along the Mediterranean seaside (Llasat, 2001; Romero et al., 1998; Peñarrocha et al., 2002). The Ebro Basin has a long record of social, economic and environmental damages caused by extreme rainfall events (García-Ruiz et al., 2000; Lasanta, 2003) due to its complex climatology, as a meteorological border region, and the contrasted relief.

## 2.2 Data base

The database consisted on 112 selected rainfall series from the Ebro Hydrographical Confederation SAIH system—Automatic Hydrological Information Network (Fig. 1). Each station provides precipitation data at a time resolution of 15 min. The system started on 1997, and is the only dense network providing sub-daily resolution data in

## Mapping rainfall erosivity at a regional scale

M. Angulo-Martínez et al.

Title Page

Abstract

Introduction

Conclusions

References

Tables

Figures

◀

▶

◀

▶

Back

Close

Full Screen / Esc

Printer-friendly Version

Interactive Discussion



the region. We used all available series data for the period 01 January 1997 to 31 December 2006.

The rainfall series were subjected to a quality control that allowed identifying wrong records due to system failures. These records were replaced by the corresponding ones from a nearby station. This allowed creating an erosive events database (EEDB). The erosive events were determined by the RUSLE criterion: an event is considered erosive if at least one of this conditions is true: i) the cumulative rainfall is greater than 12.7 mm, or ii) the cumulative rainfall has at least one peak greater than 6.35 mm in 15 min. Two consecutive events are considered different from each other if the cumulative rainfall in a period of 6 h is greater than 1.27 mm.

### 2.3 Rainfall erosivity index

The rainfall erosivity indices employed were the average  $EI_{30}$  index events and the RUSLE  $R$  factor. These indices have been widely used, making it possible to compare the results with those of other studies. The RUSLE model uses the Brown and Foster (1987) approach for calculating the average annual rainfall erosivity,  $R$  ( $\text{MJ mm ha}^{-1} \text{h}^{-1} \text{y}^{-1}$ ):

$$R = \frac{1}{n} \sum_{j=1}^n \sum_{k=1}^{m_j} (EI_{30})_k \quad (1)$$

where  $n$  is the number of years of record,  $m_j$  is the number of erosive events of a given year  $j$ , and  $EI_{30}$  is the rainfall erosivity index of a singular event  $k$ . Thus, the  $R$  factor is the average value of the annual cumulative  $EI_{30}$  over a given period. The event's rainfall erosivity  $EI_{30}$  ( $\text{MJ mm ha}^{-1} \text{h}^{-1}$ ) is obtained after dividing the event into  $o$  slices of 15 min as follows:

$$(EI_{30})_k = \left( \sum_{r=1}^o e_r v_r \right) I_{30} \quad (2)$$

## Mapping rainfall erosivity at a regional scale

M. Angulo-Martínez et al.

Title Page

Abstract

Introduction

Conclusions

References

Tables

Figures

◀

▶

◀

▶

Back

Close

Full Screen / Esc

Printer-friendly Version

Interactive Discussion



where  $e_r$  and  $v_r$  are, respectively, the unit rainfall energy ( $\text{MJ ha}^{-1} \text{mm}^{-1}$ ) and the rainfall volume (mm) during a time slice  $r$ , and  $I_{30}$  is the maximum rainfall intensity during a period of 30 min in the event ( $\text{mm h}^{-1}$ ). The unit rainfall energy,  $e_r$ , is calculated for each time slice as:

$$e_r = 0.29[1 - 0.72 \exp(-0.05i_r)] \quad (3)$$

where  $i_r$  is the rainfall intensity during the time slice ( $\text{mm h}^{-1}$ ). In addition to the  $R$  factor, we also calculated the average  $EI_{30}$  of the erosive events over the study period. The average  $EI_{30}$  complements the information given by the  $R$  factor, since it is more influenced by the events with highest erosivity than  $R$ .

## 2.4 Spatial modelling

In many studies the rainfall erosivity calculation is reduced to at-site analysis. An improvement focus on the reduction of the risk of erosion in landscape management and conservation planning is to obtain continuous maps for large areas as a preliminary step to evaluate the hazard. For this purpose a common procedure is the mapping of at-site estimated rainfall erosivity index values by means of interpolation techniques (e.g., Prudhome and Reed, 1999; Weisse and Bois, 2002).

In this article several interpolation methods including global, local and mixed approaches, are compared in order to determine which one describes better the spatial distribution of the average  $EI_{30}$  index and the  $R$  factor. A leave-one-out cross-validation technique was used for validating the goodness of fit (Efron and Tibshirani, 1997).

For the regression-based models, a digital elevation model (DEM) and a digital coverage of the Iberian Peninsula coastline were used. Both were obtained from the Ebro Hydrographical Confederation (<http://www.chebro.es/>).

## Mapping rainfall erosivity at a regional scale

M. Angulo-Martínez et al.

Title Page

Abstract

Introduction

Conclusions

References

Tables

Figures

◀

▶

◀

▶

Back

Close

Full Screen / Esc

Printer-friendly Version

Interactive Discussion



## 2.4.1 Global methods

The global method used was a multiple regression model. Regression is a global approach to spatial interpolation, and it is based on finding empirical relationships between the variable of interest and other spatial variables. Regression-based techniques adapt to almost any space and usually generate adequate maps (Goodale et al., 1998; Vogt et al., 1997; Ninyerola et al., 2000). The relationships between climatic data and topographic and geographic variables have been extensively analyzed throughout the scientific literature, and regression-based models allow exploiting this relationship to produce maps of climatic parameters. Some authors have shown the advantages of incorporating the information provided by ancillary data on mapping extreme rainfall probabilities (Beguería and Vicente-Serrano, 2006; Casas et al., 2007). Regression methods can be especially adequate in large regions with complex atmospheric influences, such as the Ebro Valley (Daly et al., 2002; Weisse and Bois, 2002; Vicente-Serrano et al., 2003), or if the sample network is not dense enough for local interpolation methods (Dirks et al., 1998).

Therefore, the average  $E/_{30}$  index and the  $R$  factor were estimated by:

$$z(x) = b_0 + \sum_1^n b_n P_n(x) + \varepsilon(x) \quad (4)$$

where  $z$  is the predicted value of the parameter at a given location  $x$ ,  $b_0$  to  $b_n$  are regression coefficients,  $P_1$  to  $P_n$  are spatially distributed independent variables, and  $\varepsilon$  is a normally distributed, random error.

We used a set of independent variables at a spatial resolution of 100 m (Table 1). Elevation is usually the main determinant of the spatial distribution of climatic variables. Nevertheless, other variables such as the latitude and longitude, the distance to the oceans or the incoming solar radiation may also have an influence on the distribution of erosive rains. Most variables were derived from a DEM (UTM-30N coordinates), except the distance to the Cantabrian and Mediterranean seas which were obtained from

## HESSD

6, 417–453, 2009

### Mapping rainfall erosivity at a regional scale

M. Angulo-Martínez et al.

Title Page

Abstract

Introduction

Conclusions

References

Tables

Figures

◀

▶

◀

▶

Back

Close

Full Screen / Esc

Printer-friendly Version

Interactive Discussion



## Mapping rainfall erosivity at a regional scale

M. Angulo-Martínez et al.

Title Page

Abstract

Introduction

Conclusions

References

Tables

Figures



Back

Close

Full Screen / Esc

Printer-friendly Version

Interactive Discussion



the Iberian Peninsula coastline coverage. The incoming solar radiation is a spatially continuous variable that depends on the terrain aspect (northern and southern slopes have low and high incoming solar radiation values, respectively). The annual mean incoming solar radiation was calculated following the algorithm of Pons and Ninyerola (2008). All these variables were processed in the MiraMon GIS package (Pons, 2006). Low-pass filters with radii of 5, 10 and 25 km were applied to elevation, slope and incoming solar radiation in order to measure the widest influence of these variables.

For the model selection (identification of the significant variables) we used a forward stepwise method based on the Akaike's Information Criterion (Venables and Ripley, 2002). A ten-fold cross-validation procedure was used, consisting in repeating the stepwise method ten times, each time leaving one tenth of the sample out of the analysis (Breiman and Spector, 1992). In an ideal case all ten repetitions should yield the same set of significant variables, what is an indication of a reliable model. To avoid excessive influence of outlier observations which were present in the data, a robust regression procedure was used consisting in assigning a weight to each observation which was inversely proportional to its influence on the model fitting process (Marazzi, 1993). The R statistical analysis package (R Development Core Team, 2008) was used for the regression analysis.

### 2.4.2 Local methods

In global methods, local variations are dismissed as random, unstructured noise, and the climatic map is created on the basis of general structure of the variable at all available points (Borough and McDonnell, 1998). Local methods, on the contrary, use only the data of the nearest sampling points for climatic mapping. Since interpolated values at ungauged locations depend on the observed values, local methods strongly depend on a sufficiently dense and evenly spaced sampling network.

Two local methods were used: inverse distance weighting (IDW) and splines. The IDW interpolation is based on the assumption that the climatic value at an unsampled point  $z(x)$  is a distance-weighted average of the climatic values at nearby sampling

points  $z(x_1), z(x_2), \dots, z(x_n)$ . Climatic values are more similar at closer distances, so the inverse distance ( $1/d_j$ ) between  $z(x_i)$  and  $z(x)$  is used as the weighting factor:

$$z(x) = \frac{\sum_{i=1}^n z(x_i) d_{ij}^{-r}}{\sum_{i=1}^n d_{ij}^{-r}} \quad (5)$$

where  $z(x)$  is the predicted value,  $z(x_i)$  is the climatic value at a neighbouring weather station,  $d_{ij}$  is the distance between  $z(x)$  and  $z(x_i)$ , and  $r$  is an empirical parameter. Models with  $r=1$ ,  $r=2$  and  $r=3$  were tested.

The splines method is based on a family of continuous, regular and derivable functions. Splines are similar to the equations obtained from the trend surfaces or regression-based methods, but they are fitted locally from the neighbouring points around the candidate location  $x$ . A new function is created for each location  $x$ , without lost of continuity properties among the curves. Smoothing or tension parameters can be specified, resulting in more or less smoothed maps. The predicted value  $z(x)$  is determined by two terms:

$$z(x) = T(x) + \sum_{i=1}^n \lambda_j \psi_j(r_i) \quad (6)$$

where  $T(x)$  is a polynomial smoothing term, and the second term groups a series of radial functions where  $\psi_j(r_i)$  is a known group of functions, and  $\lambda_j$  represents the parameters (Mitasova et al., 1995):

$$\psi(r_i) = - \left[ \ln \left( \frac{\varphi \times r_i}{2} \right) + E_i \left( \frac{\varphi \times r_i}{2} \right) + C_E \right] \quad (7)$$

where  $\varphi$  is the tension coefficient,  $C_E=0.577215\dots$  is the Euler constant,  $E_i$  is the exponential integral function, and  $r_i$  is:

$$r_i = \sqrt{(x - x_i)^2 + (y - y_i)^2} \quad (8)$$

## Mapping rainfall erosivity at a regional scale

M. Angulo-Martínez et al.

Title Page

Abstract

Introduction

Conclusions

References

Tables

Figures

◀

▶

◀

▶

Back

Close

Full Screen / Esc

Printer-friendly Version

Interactive Discussion



The algorithms for fitting splines are quite complex but are currently standard in GIS packages. In this paper several spline interpolations were used as implemented in the ArcGIS 9.2 software. Tension and smoothing parameters were  $\varphi=400$ ,  $\varphi=5000$ ,  $T(x)=0$  and  $T(x)=400$ .

Geostatistical interpolation methods (or kriging) assume that the spatial variation of a continuous climatic variable is too irregular to be modelled by a continuous mathematical function, and its spatial variation could be better predicted by a probabilistic surface. This continuous variable is called a regionalized variable, which consists of a drift component and a random but spatially correlated component (Borough and McDonnell, 1998). The spatially located climatic variable  $z(x)$  is expressed by:

$$z(x) = m(x) + \varepsilon'(x) + \varepsilon'' \quad (9)$$

where  $m(x)$  is the drift component that indicates the structural variation of the climatic variable and  $\varepsilon'(x)$  are the residuals, the difference between the drift component and the sampling data values. These residuals are spatially dependent, whereas  $\varepsilon''(x)$  indicates the spatially independent residual. The predictions of kriging-based methods are currently a weighted average of the data available at neighbouring weather stations. The weighting is chosen so that the calculation is not biased and the variance is minimal. Initially, a function that relates the spatial variance of the climatic variable must be determined using a semi-variogram model which relates the semi-variances between the climatic values at different spatial distances.

There are different types of kriging and several sources describe them in detail (see, for example, Isaaks and Strivastava, 1989; Goovaerts, 1997; Borough and McDonnell, 1998). In this paper the geostatistical methods used were simple kriging, ordinary kriging, ordinary kriging with anisotropy and co-kriging, as implemented in the ArcGIS 9.2 software.

## Mapping rainfall erosivity at a regional scale

M. Angulo-Martínez et al.

Title Page

Abstract

Introduction

Conclusions

References

Tables

Figures

◀

▶

◀

▶

Back

Close

Full Screen / Esc

Printer-friendly Version

Interactive Discussion



### 2.4.3 Mixed methods

Mixed methods are based on a combination of regression and local interpolation techniques, exploiting the ability of regression to relate the target variable to other spatially distributed variables and the spatial self-correlation acting at the local scale on most spatial variables. Alternative forms of mixed methods have been proposed in the last years for mapping environmental variables (Brown and Comrie, 2002; McBratney et al., 2003; Ninyerola et al., 2007; Vicente-Serrano et al., 2007). These and other studies have demonstrated that mixed methods usually allow for more precise and detailed representations of the target variables.

In this study, the residuals  $\varepsilon$  in Eq. (4) were obtained after applying the regression model to the observed values, and values were then interpolated using a local method. Inverse distance weighting with  $r=2$ , splines with tension with  $\varphi=400$  and ordinary kriging were used. The final prediction of the mixed model is the sum of the values predicted by the regression model and the interpolated residuals.

### 2.5 Validation

The resulting maps were compared by using a set of validation statistics comparing the predicted and the observed values of the  $R$  factor and the  $EI_{30}$  index. A leave-one-out procedure was used, consisting in fitting the model  $n-1$  times –  $n$  being the number of observations in the data set –, each time one observation is left out of the fitting sample. These observations are used to calculate the model residuals, i.e. the difference between the predicted and the observed values. Cross-validation techniques are preferred to more traditional split-sample procedures for estimating generalization error, since they allow an independent validation without sacrificing an important amount of data (Weiss and Kulikowski, 1991). Cross-validation is compulsory when comparing exact interpolators such as IDW or splines, which by definition give an exact value at the locations for which there are observations, i.e. all residuals by these models are zero.

## Mapping rainfall erosivity at a regional scale

M. Angulo-Martínez et al.

Title Page

Abstract

Introduction

Conclusions

References

Tables

Figures

◀

▶

◀

▶

Back

Close

Full Screen / Esc

Printer-friendly Version

Interactive Discussion



**Mapping rainfall erosivity at a regional scale**

M. Angulo-Martínez et al.

Title Page

Abstract

Introduction

Conclusions

References

Tables

Figures



Back

Close

Full Screen / Esc

Printer-friendly Version

Interactive Discussion



We used a set of goodness of fit statistics not to rely on a single one (Table 2). These include the coefficient of determination ( $r^2$ ) of the regression between the predicted and the observed values, as well as the intercept and slope parameters of the regression line as an indicator of bias in the predictions. Two error statistics were also computed: i) the mean bias error (MBE), which is centred around zero and is an indicator of prediction bias; and ii) the mean absolute error (MAE), which is a measure of the average error. We avoided using the root mean square error (RMSE) because it is highly biased by outlier observations, and also because it is difficult to discern whether it reflects the average error or the variability of the squared errors (Willmott and Matsuura, 2005). Finally, we computed the agreement index  $D$  (Willmott, 1981), which scales the magnitude of the variables, retains mean information and does not amplify the outliers.

**3 Results**

All interpolation methods were able to capture the regional distribution of the two rainfall erosivity parameters (Figs. 2 and 3). The  $R$  factor was highest – from 1200 to 4500 MJ mm ha<sup>-1</sup> h<sup>-1</sup> y<sup>-1</sup> – in two areas: i) in the Pyrenees Range at the north, especially in the central part; and ii) in the south-east mountainous part, corresponding to the Iberian Range and the southern east region. The lowest values – from 40 to 800 MJ mm ha<sup>-1</sup> h<sup>-1</sup> y<sup>-1</sup> – appeared in the north-west of the area and in the centre of the Ebro River valley. The spatial distribution of the  $EI_{30}$  index was slightly different, showing a clear gradient from the north-west (Cantabric Sea) to the south-east (Mediterranean Sea), modified to a certain extent by the relief. The highest values – from 70 to 190 MJ mm ha<sup>-1</sup> h<sup>-1</sup> – were found in the south-east corner, along the coast. Lower values – from 8 to 40 MJ mm ha<sup>-1</sup> h<sup>-1</sup> – are found close to the Cantabric Sea. This pattern is similar to the distribution of the extreme rainfall events in the region (Beguiría et al., 2008), and is an indicator of the  $EI_{30}$  index being closely related to the most intense rainfall events.

**Mapping rainfall erosivity at a regional scale**

M. Angulo-Martínez et al.

Title Page	
Abstract	Introduction
Conclusions	References
Tables	Figures
◀	▶
◀	▶
Back	Close
Full Screen / Esc	
Printer-friendly Version	
Interactive Discussion	



The spatial distribution of both indices over the study area can be explained to a large extent by the proximity to – or isolation from – the water masses (the Cantabrian and Mediterranean seas). The relief, with mountain ranges to the north, south and east of the region, modify this general pattern by increasing rainfall in those areas. Another effect of the relief is the isolation of the central area from the main precipitation sources, i.e. creating a zone of rain shadow.

Despite the general spatial pattern, differences were evident between the models. The maps produced by the local methods – IDW and Spline with tension – were very much linked to individual observations, resulting excessively local. In most cases, local variance can be associated with the occurrence of anomalous events or very specific conditions, and might not reflect the general pattern adequately. The maps produced by these two methods varied slightly depending on the value of the  $r$  and  $\rho_{\psi}$  parameters (maps not shown), but in all cases they had this characteristic. The smoothed splines method, which includes a smoothing function to reduce excessive influence of local observations, produced a more regularized output.

Geostatistical methods (simple kriging, ordinary kriging with anisotropy and co-kriging) produced much more smoothed results than the local methods, yet retaining a good degree of detail. Differences between the three methods were few, although an increasing degree of local detail was found from the simplest to the most complex method. It can be noticed that simple kriging gave higher values for the centre of the valley, overestimating the model.

Regression produced the smoothest result, as a consequence of being a purely global method. The independent variables selected by the stepwise procedure were ELEV, MED and CANTAB for  $R$  and LON, LAT, MED and RAD for  $EI_{30}$  (Table 3). The selection of variables was remarkably constant during the jackknife process, confirming the statistical significance of these variables. However the uncertainty of the prediction is reflected by the relatively low determination coefficient (Table 3). For both  $R$  and  $EI_{30}$  the location variables (distance to the sea and longitude) were the most influential, followed by the topographic variables (elevation and radiation), as shown by

the standardized coefficients (Table 4). The map resulting from the regression model (Figs. 2 and 3) did not show as higher values as the other methods, especially at the south-east of the study area where the maximum values of both  $R$  and  $EI_{30}$  were observed. This fact can be explained by the use of a weighted regression model, which underestimates the importance of outlier observations during the fitting process.

The maps obtained by mixed methods (regression plus local interpolation of the model residuals) had an increased degree of local detail, and corrected the underestimation problem of the regression model alone. The maps produced by mixed methods reflected better the local diversity than any other method alone, whereas maintaining the general pattern. The high level of visual detail on these maps makes them more appealing to the viewer, what enhances communication.

Tables 5 and 6 summarize the statistics of the predicted variables and the validation parameters. All methods underestimated the variance of the  $R$  and  $EI_{30}$  indices, resulting in relatively poor predictions. The observed standard deviation was 621.7 for the  $R$  factor, which varied in the range 40–4500 MJ mm ha<sup>-1</sup> h<sup>-1</sup> y<sup>-1</sup>, and 23.8 for  $EI_{30}$ , which varied in the range 8–190 MJ mm ha<sup>-1</sup> h<sup>-1</sup>. Compared with that, the standard deviation of the estimations ranged between 228.4 and 420.4 for  $R$  and 8.7 and 16.2 for  $EI_{30}$  (Tables 5 and 6). Consequently, all models had relatively large absolute errors, which were higher than 30% of the mean predicted value for most of them. Similarly, the  $r^2$  and Willmott's  $D$  values were relatively low. The low performance was mostly due to the inability to predict the highest values, especially those above 2000 MJ mm ha<sup>-1</sup> h<sup>-1</sup> y<sup>-1</sup> for  $R$  and 100 MJ mm ha<sup>-1</sup> h<sup>-1</sup> for  $EI_{30}$ , respectively (Figs. 4 and 5). The large uncertainty of the predictions can be attributed to the high random variability of both erosivity indices in the study area and during the study period. In fact, during an initial inspection of the data set it was apparent that close observatories could have very different values of  $R$  and  $EI_{30}$ .

Differences between the models regarding the validation statistics were narrow, but allowed for a comparison. The mixed methods offered the best results overall, from their visual appearance and the validation results. Other models as ordinary kriging

## Mapping rainfall erosivity at a regional scale

M. Angulo-Martínez et al.

Title Page

Abstract

Introduction

Conclusions

References

Tables

Figures

◀

▶

◀

▶

Back

Close

Full Screen / Esc

Printer-friendly Version

Interactive Discussion



with anisotropy and IDW method with  $r=3$  for the  $R$  factor were equally good according to the  $r^2$ , the Willmott's  $D$  statistic and MBE, and also had one of the lowest MAE. For the  $EI_{30}$  index, the regression model plus splines with tension interpolated residuals had the highest  $r^2$  and also the lowest MBE. The Willmott's  $D$  statistics favoured the regression model plus IDW interpolated residuals, followed by the rest of the mixed models, ordinary kriging with anisotropy and splines with tension.

#### 4 Discussion and conclusions

Rainfall erosivity is an indicator of the precipitation aggressiveness, and depends on the rainfall energy (raindrop size distribution and kinetic energy) and the intensity of the storm event. Rainfall under Mediterranean climate is characterized by high temporal variability and a flashy character. This last characteristic affects especially the rainfall erosivity, which depends on the occurrence of few, very intense, events (González-Hidalgo et al., 2007).

In this study we used the RUSLE  $R$  factor and the average  $EI_{30}$  index of the erosive events to assess the spatial distribution of rainfall erosivity on the north-eastern Iberian Peninsula. Both variables are characterized by a high temporal variability, especially in the Mediterranean area and in geographically complex regions (Leek and Olsen 2000; González-Hidalgo et al., 2007). During the initial stage of the analysis it was evident that close observatories could have very different values of  $R$  and  $EI_{30}$ . Nevertheless, obtaining robust spatially continuous models of rainfall erosivity is interesting in itself, but also as a needed step for its integration into erosion models.

Comparing both erosivity indices, the average  $EI_{30}$  index of the erosive events had larger variability than  $R$ , being more affected by the most extreme events. The spatial pattern of  $EI_{30}$  showed a clear northwest-southeast gradient. The highest values were found in the southern region, coinciding with the distribution of the peak intensity of extreme rainfall events for the same area (Beguería et al., 2008). The spatial distribution of the  $R$  factor showed the highest values in the north and the south-east part,

## Mapping rainfall erosivity at a regional scale

M. Angulo-Martínez et al.

Title Page

Abstract

Introduction

Conclusions

References

Tables

Figures

◀

▶

◀

▶

Back

Close

Full Screen / Esc

Printer-friendly Version

Interactive Discussion



isolating the centre of the valley with low values. Previous works have analyzed the spatial distribution of the USLE  $R$  factor in Spain (ICONA, 1988). The value range and the spatial distribution are similar to the results of our study. There are differences however in the south-east corner along the Mediterranean coastland. The map of ICONA (1988) did not show the high erosivity values which were presented in our dataset. This discrepancy could be due to the different period of analysis, since the study of ICONA (1988) was based on data from the period 1966–1976, although this issue could not be assessed using the current dataset. Unfortunately, the technical brief attached to the map of ICONA did not report enough details allowing for a deeper comparison. The  $R$  factor values found for the area are similar to the ones published by other authors for the Mediterranean region: 697.4 to 3741.8 MJ mm ha<sup>-1</sup> h<sup>-1</sup> y<sup>-1</sup> in Portugal (De Santos Loureiro and De Azevedo Coutinho, 2001); 471 and 3214 MJ mm ha<sup>-1</sup> h<sup>-1</sup> y<sup>-1</sup> in Italy (Diodato, 2004); 339 to 818 MJ mm ha<sup>-1</sup> h<sup>-1</sup> y<sup>-1</sup> in central Spain (Boellstorff and Benito, 2005); or 419.01 to 1124.36 MJ mm ha<sup>-1</sup> h<sup>-1</sup> y<sup>-1</sup> in Sicily (Onori et al., 2006). We are not aware of previous studies analyzing the spatial distribution of the average  $EI_{30}$  index in the literature.

Despite the high spatial variability of both indices, the mapping methods tested were able to capture the main spatial pattern of rainfall erosivity in the area. The spatial distribution can be explained by seasonal atmospheric behaviour which causes the major stormy events. In the Pyrenees these events are related with south western flows confronting the mountains triggering orographic rainfall in winter, and convective storms in summer. Close to the Mediterranean Sea the heating contrast between the atmosphere upper levels and continental and maritime surfaces, more intense during fall, generates intense storms. This is the principal cause of heavy rainfalls in the southeastern area (Llasat and Puigcerver, 1997). These synoptic situations explain the spatial pattern of rainfall erosivity, which is linked to the most extreme events of the year. In addition, the strong relief adds complexity to the climate dynamics making more complex to obtain reliable models. It is responsible of orographic precipitation increase, and it also generates temperature differences in narrow spaces which contribute to the

## Mapping rainfall erosivity at a regional scale

M. Angulo-Martínez et al.

Title Page

Abstract

Introduction

Conclusions

References

Tables

Figures

◀

▶

◀

▶

Back

Close

Full Screen / Esc

Printer-friendly Version

Interactive Discussion



formation of convective cellules and local storms. Thus, all rainfall erosivity maps show a clear north-west to south-east gradient, and marked local differences caused by the relief.

The comparison of several interpolation techniques yielded mixed results, since no single method arose as the best one according to all validation metrics. The Willmott's  $D$  statistic tended to favour the use of regression plus inverse distance weighting residuals for both  $R$  and  $EI_{30}$ , although other methods such as ordinary kriging with anisotropy or IDW also ranked well. This result coincides with the common assumption that mixed methods (global regression plus local interpolation of the model residuals) are best for generating surfaces of climatic variables (Brown and Comrie, 2002; Vicente-Serrano et al., 2003; McBratney et al., 2003; Ninyerola et al., 2007; He et al., 2007). Beyond the validation statistics, only regression-based techniques provide a means of testing hypothesis about the influence of geographical variables on the variable of interest. In our case, they allowed quantify the influence of the distance to the coast and the elevation on rainfall erosivity, a fact that has been also described by other authors (Goovaerts, 1999; Van Dijk et al. 2002; Domínguez-Romero et al., 2007).

In general, the models were bad at predicting the highest values of both indices, due to the presence of outlier observations. This problem affected the process of variable selection in the regression models, and recommended the use of a robust regression procedure which minimizes the importance of outlier observations in the fitting process. This in turn penalized regression-based models on the comparison, since most validation statistics are highly influenced by misrepresentation of the most extreme observations. The uncertainty of the predicted values can be explained by the natural climate variability in the study area, and also by the length of the analysis period. Other authors have reported high variability of soil erosion values in the Mediterranean region, both in space and time (González-Hidalgo et al., 2007). With respect to the length of the data series, it is generally accepted that a minimum of 20 years is desirable for rainfall erosivity analysis (Renard and Freimund, 1994; Renard et al., 1997; Curse et al., 2006; Verstraeten et al., 2006). Unfortunately, there are very few data

## Mapping rainfall erosivity at a regional scale

M. Angulo-Martínez et al.

Title Page

Abstract

Introduction

Conclusions

References

Tables

Figures

◀

▶

◀

▶

Back

Close

Full Screen / Esc

Printer-friendly Version

Interactive Discussion



bases of high time resolution rainfall records and a good spatial coverage, as the one used in this work. Regarding to this character, the maps obtained by the local methods were the most influenced by the high variability of the erosivity indices, masking the general spatial pattern. Longer series are needed for reducing the spatial noise.

5 The availability of high-quality environmental maps is a key issue for agricultural and hydrological management in many regions of the World. Rainfall erosivity maps can be of high relevance as a guidance for soil conservation practices, and also because they are usually part of erosion models such as the RUSLE. Recently, the RUSLE model has been implemented into GIS packages, integrating all the factors as different layers. Hence, the accuracy of the spatial surface of each factor is propagated to the outputs of the model. Compared to other climatic variables, rainfall erosivity is characterized by a high spatial and inter-annual variability, what makes mapping more difficult. However, we have found that reasonable results can be found by using several spatial interpolation techniques. Between the several methodologies tested, we found that mixed models (multiple regression plus local interpolation of the residuals) yielded the highest level of spatial detail, and also ranked highest using several validation statistics. The use of regression techniques allowed also assessing the statistical significance of geographical variables influencing the distribution of rainfall erosivity. Validation of the models showed that there is still uncertainty in the prediction of rainfall erosivity, which can be attributed to the high spatial and temporal variability of this parameter and the importance of outlier observations in the data series.

20 Further research may be directed to find reliable erosivity indices which can be computed from daily precipitation data. This would allow using daily precipitation data bases, which are usually longer and have a higher spatial coverage. This would lead to more robust results, and will also make trend analysis possible.

25 *Acknowledgements.* We want to express our gratitude to the Ebro River Hydrographical Confederation (Confederación Hidrográfica del Ebro – CHE) for providing the data used on this study. This work has been supported by the research projects CGL2008-00831/BTE, CGL2005-04508/BOS and CGL2008-01189/BTE, funded by the Spanish Ministry of Science

---

## Mapping rainfall erosivity at a regional scale

M. Angulo-Martínez et al.

---

Title Page

Abstract

Introduction

Conclusions

References

Tables

Figures



Back

Close

Full Screen / Esc

Printer-friendly Version

Interactive Discussion



and Innovation. Research of M.A. is supported by a JAE-Predoc Research Grant from the Spanish National Research Council (Consejo Superior de Investigaciones Científicas – CSIC).

## References

- Arnoldus, H. M. J.: Methodology used to determine the maximum potential average annual soil loss due to sheet and rill erosion in Morocco, *FAO Soils Bull.*, 34, 39–51, 1977.
- Beguería, S., Vicente-Serrano, S. M., López-Moreno, J. I., and García-Ruiz, J. M.: Annual and seasonal mapping of peak intensity, magnitude and duration of extreme precipitation events across a climatic gradient, North-east Iberian Peninsula, *Int. J. Climatol.*, in press, 2008.
- Beguería, S. and Vicente-Serrano, S. M.: Mapping the hazard of extreme rainfall by peaks over threshold extreme value analysis and spatial regression techniques, *J. Appl. Meteorol.*, 45, 108–124, 2006.
- Boellstorff, D. and Benito, G.: Impacts of set-aside policy on the risk of soil erosion in central Spain, *Agr. Ecosyst. Environ.*, 107, 231–243, 2005.
- Borough, P. A. and McDonnell, R. A.: *Principles of Geographical Information Systems*, Oxford University Press, USA, 1998.
- Breiman, L. and Spector, P.: Submodel selection and evaluation in regression: The X-random case, *Int. Stat. Rev.*, 60, 291–319, 1992.
- Brown, D. P. and Comrie, A. C.: Spatial modelling of winter temperature and precipitation in Arizona and New Mexico, USA, *Climate Res.*, 22, 115–128, 2002.
- Brown, L. C. and Foster, G. R.: Storm erosivity using idealized intensity distributions. *T. ASAE.*, 30, 379–386, 1987.
- Casas, M. C., Herrero, M., Ninyerola, M., Pons, X., Rodríguez, R., Rius, A., and Redaño, A.: Analysis and objective mapping of extreme daily rainfall in Catalonia, *Int. J. Climatol.*, 27, 399–409, 2007.
- Creus, J.: *Las sequías en el valle del Ebro*, edited by: Gil, A. and Morales, A., *Causas y consecuencias de las sequías en España*, Universidad D’Alacant, 231–259, 2001.
- Cuadrat, J. M.: *Las sequías en el valle del Ebro. Aspectos climáticos y consecuencias económicas*, *Rev. Real Acad. Cien.*, 85, 537–545, 1991.
- Curse, R., Flanagan, J., Frankenberger, B., Gelder, D., Herzmann, D., James, D., Krajenski, W.,

# HESSD

6, 417–453, 2009

## Mapping rainfall erosivity at a regional scale

M. Angulo-Martínez et al.

Title Page

Abstract

Introduction

Conclusions

References

Tables

Figures

◀

▶

◀

▶

Back

Close

Full Screen / Esc

Printer-friendly Version

Interactive Discussion



## Mapping rainfall erosivity at a regional scale

M. Angulo-Martínez et al.

Title Page

Abstract

Introduction

Conclusions

References

Tables

Figures



Back

Close

Full Screen / Esc

Printer-friendly Version

Interactive Discussion



- Kraszewski, M., Laflen, J., Opsomer, J., and Todey, D.: Daily estimates of rainfall, water runoff and soil erosion in Iowa, *J. Soil Water Conserv.*, 61, 191–199, 2006.
- Daly, C., Gibson, W. P., Taylor, G. H., Johnson, G. L., and Pasteris, P.: A knowledge-based approach to the statistical mapping of climate, *Climate Res.*, 22, 99–113, 2002.
- 5 Diodato, N.: Estimating RUSLE's rainfall factor in the part of Italy with a Mediterranean rainfall regime, *Hydrol. Earth Syst. Sci.*, 8, 103–107, 2004, <http://www.hydrol-earth-syst-sci.net/8/103/2004/>.
- Dirks, K. N., Hay, J. E., Stow, C. D., and Harris D.: High-resolution studies of rainfall on Norfolk Island, Part II: Interpolation of rainfall data, *J. Hydrol.*, 208, 187–193, 1998.
- 10 Domínguez-Romero, L., Ayuso Muñoz, J. L., and García Marín, A. P.: Annual distribution of rainfall erosivity in western Andalusia, southern Spain, *J. Soil Water Conserv.*, 62, 390–401, 2007.
- Dunkerley, D.: Rain event properties in nature and in rainfall simulation experiments: a comparative review with recommendations for increasingly systematic study and reporting, *Hydrol. Process.*, 22, 4415–4435, doi:10.1002/hyp.7045, 2008.
- Efron, B. and Tibshirani, R. J.: Improvements on cross-validation: the .632+ bootstrap method, *J. Am. Stat. Assoc.*, 92, 548–560, 1997.
- García-Ruiz, J. M., Arnáez, J., White, S. M., Lorente, A., and Beguería, S.: Uncertainty assessment in the prediction of extreme rainfall events: an example from the Central Spanish Pyrenees, *Hydrol. Process.*, 14, 887–898, 2000.
- 20 Garrido, J. and García, J. A.: Periodic signals in Spanish monthly precipitation data, *Theor. Appl. Climatol.*, 45, 97–106, 1992.
- Gobin, A., Jones, R., Kirkby, M., Campling, P., Govers, G., Kosmas, C., and Gentile, A. R.: Indicators for pan-European assessment and monitoring of soil erosion by water, *Environ. Sci. Policy*, 7, 25–38, 2004.
- 25 González-Hidalgo, J. C., Peña-Monnè, J. L., and de Luis, M.: A review of daily soil erosion in western Mediterranean areas, *Catena*, 71, 193–199, 2007.
- Goodale, C. L., Aber, J. D., and Ollinger, S. V.: Mapping monthly precipitation, temperature and solar radiation from Ireland with polynomial regression and a digital elevation model, *Climate Res.*, 10, 35–49, 1998.
- 30 Goovaerts, P.: Using elevation to aid the geostatistical mapping of rainfall erosivity, *Catena*, 34, 227–242, 1999.
- Goovaerts, P.: *Geostatistics for Natural Resources Evaluation*, Oxford University Press, New

York, 1997.

He, H., Guo, Z., and Xiao, W.: Review on spatial interpolation techniques of rainfall, Chinese J. Ecol., 24, 1187–1191, 2005.

Hoyos, N., Waylen, P. R., and Jaramillo, A.: Seasonal and spatial patterns of erosivity in a tropical watershed of the Colombian Andes, J. Hydrol., 314, 177–191, 2005.

Hudson, N.: Soil Conservation, Cornell University Press, Ithaca, 1971.

Kinnell, P. I. A. and Risse, L. M.: USLE-M: Empirical modelling rainfall erosion through runoff and sediment concentration, Soil Sci. Soc. Am. J., 62, 1667–1672, 1998.

ICONA.: Agresividad de la lluvia en España. Valores del factor R de la Ecuación Universal de Pérdida de Suelo, Ministerio de Agricultura, pesca y alimentación, España, 1988.

Isaaks E. H. and Strivastava, R. M.: An Introduction to Applied Geostatistics, Oxford University Press, Oxford, 1989.

Lal, R.: Soil erosion on alfisols in Western Nigeria. III – Effects of rainfall characteristics, Geoderma, 16, 389–401, 1976.

Lana, X. and Burgueño, A.: Spatial and temporal characterization of annual extreme droughts in catalonia (Northeast Spain), Int. J. Climatol., 18, 93–110, 1998.

Lasanta, T.: Gestión agrícola y erosión del suelo en la cuenca del Ebro: el estado de la cuestión, Zubía, 21, 76–96, 2003.

Llasat, M. C.: An objective classification of rainfall events on the basis of their convective features: Application to rainfall intensity in the northeast of Spain, Int. J. Climatol., 21, 1385–1400, 2001.

Llasat, M. C. and Puigcerver, M.: Meteorological factors associated with floods in the north-eastern part of the Iberian Peninsula, Nat. Hazards, 5, 133–151, 1994.

Leek, R. and Olsen, P.: Modelling climatic erosivity as a factor for soil erosion in Denmark: changes and temporal trends, Soil Use Manage., 16, 61–65, 2000.

Lim, K. J., Sagong, M., Engel, B. A., Tang, Z., Choi, J., and Kim, K.: GIS-based sediment assessment tool, Catena, 64, 61–80, 2005.

López-Vicente, M., Navas, A., and Machin, J.: Identifying erosive periods by using RUSLE factors in mountain fields of the Central Spanish Pyrenees, Hydrol. Earth Syst. Sci., 12, 523–535, 2008,  
<http://www.hydrol-earth-syst-sci.net/12/523/2008/>.

McBratney, A., Mendonça-Santos, M., and Minasny, B.: On digital soil mapping, Geoderma, 117, 3–52, 2003.

**HESSD**

6, 417–453, 2009

---

## Mapping rainfall erosivity at a regional scale

M. Angulo-Martínez et al.

---

Title Page

Abstract

Introduction

Conclusions

References

Tables

Figures

◀

▶

◀

▶

Back

Close

Full Screen / Esc

Printer-friendly Version

Interactive Discussion



- Marazzi, A.: Algorithms, Routines and S Functions for Robust Statistics, Wadsworth & Brooks, Cole, 1993.
- Martín-Vide, J.: Diez características de la pluviometría española decisivas en el control de la demanda y el uso del agua, B. Asoc. Geogr. Esp., 18, 9–16, 1994.
- 5 Millward, A. A. and Mersey, J. E.: Adapting the RUSLE to model soil erosion potential in a mountainous tropical watershed, Catena, 38, 109–129, 1999.
- Mitasova H., Mitas, L., Brown, W. M., Gerdas, D. P., Kosinovsky, I., and Baker, T.: Modelling spatially and temporally distributed phenomena: new methods and tools for GRASS GIS, Int. J. Geogr. Inf. Syst., 9, 433–446, 1995.
- 10 Mutua, B. M., Klik, A., and Loiskandl, W.: Modeling soil erosion and sediment yield at a catchment scale: the case of masinga catchment, Kenya, Land Degrad. Dev., 17, 557–570, 2006.
- Ninyerola, M., Pons, X., and Roure, J. M.: Monthly precipitation mapping of the Iberian Peninsula using spatial interpolation tools implemented in a Geographic Information System, Theor. Appl. Climatol., 89, 195–209, 2007.
- 15 Ninyerola, M., Pons, X., and Roure, J. M.: Objective air temperature mapping for the Iberian Peninsula using spatial interpolation and GIS, Int. J. Climatol., 27, 1231–1242, 2007.
- Ninyerola, M., Pons, X., and Roure, J. M.: A methodological approach of climatological modelling of air temperature and precipitation through GIS techniques, Int. J. Climatol., 20, 1823–1841, 2000.
- 20 Onori, F., De Bonis, P., and Grauso, S.: Soil erosion prediction at the basin scale using the revised universal soil loss equation (RUSLE) in a catchment of Sicily (southern Italy), Environ. Geol., 50, 1129–1140, doi:10.1007/S00254-006-0286-1, 2006.
- Peñarrocha, D., Estrela, M. J., and Millán, M.: Classification of daily rainfall patterns in a Mediterranean area with extreme intensity levels: the Valencia region, Int. J. Climatol., 22, 677–695, 2002.
- 25 Pons, X. and Ninyerola, M.: Mapping a topographic global solar radiation model implemented in a GIS and calibrated with ground data, Int. J. Climatol., 28, 1821–1834, doi:10.1002/joc.1676, 2008.
- Pons X.: Manual of miramon. Geographic Information System and Remote Sensing Software, Centre de Recerca Ecologica i Aplicacions Forestals (CREAF): Bellaterra, (available online: <http://www.creaf.uab.es/miramón>), 2006.
- 30 Prudhome, C. and Reed, D. W.: Mapping extreme rainfall in a mountainous region using geostatistical techniques: A case study in Scotland, Int. J. Climatol., 19, 1337–1356, 1999.

## Mapping rainfall erosivity at a regional scale

M. Angulo-Martínez et al.

Title Page

Abstract

Introduction

Conclusions

References

Tables

Figures

◀

▶

◀

▶

Back

Close

Full Screen / Esc

Printer-friendly Version

Interactive Discussion



- R Development Core Team: R: A Language and Environment for Statistical Computing, Vienna (Austria), R Foundation for Statistical Computing, 2008.
- Renard, K. G., Foster, G. R., Weesies, G. A., McCool, D. K., and Yoder, D. C.: Predicting Soil Erosion by Water: A Guide to Conservation Planning with the Revised Universal Soil Loss Equation (RUSLE). Handbook #703, US Department of Agriculture, Washington, DC., 1997.
- Renard, K. G. and Freimund, J. R.: Using monthly precipitation data to estimate the  $R$  factor in the revised USLE, *J. Hydrol.*, 157, 287–306, 1994.
- Romero, R., Guijarro, J. A., Ramis, C., and Alonso, S.: A 30-year (1964–1993) daily rainfall data base for the Spanish Mediterranean regions: first exploratory study, *Int. J. Climatol.*, 18, 541–560, 1998.
- De Santos Loureiro, N. and De Azevedo Coutinho, M.: A new procedure to estimate the RUSLE  $E/_{30}$  index, based on monthly rainfall data and applied to the Algarve region, Portugal, *J. Hydrol.*, 250(1–4), 12–18, doi:10.1016/S0022-1694(01)00387-0, 2001.
- Shi, Z. H., Cai, C. F., Ding, S. W., Wang, T. W., and Chow, T. L.: Soil conservation planning at the small watershed level using RUSLE with GIS, *Catena*, 55, 33–48, 2004.
- Van Dijk, A. I. J. M., Bruijnzeel, L. A., and Rosewell, C. J.: Rainfall intensity – kinetic energy relationships: a critical literature appraisal, *J. Hydrol.*, 261, 1–23, 2002.
- Venables, W. N. and Ripley, B. D.: *Modern Applied Statistics with S*, Fourth edition, Springer, USA, 2002.
- Verstraeten, G., Poesen, J., Demarée, G., and Salles, C.: Long-term (105 years) variability in rain erosivity as derived from 10-min rainfall depth data for Ukkel (Brussels, Belgium): implications for assessing soil erosion rates, *J. Geophys. Res.*, 111, 1–11, doi:10.1029/2006JD007169, 2006.
- Vicente-Serrano, S. M., Saz-Sánchez, M. A., and Cuadrat, J. S.: Comparative analysis of interpolation methods in the middle Ebro Valley (Spain): application to annual precipitation and temperature, *Climate Res.*, 24, 161–180, 2003.
- Vicente-Serrano, S. M.: *Las sequías climáticas en el valle medio del Ebro: factores atmosféricos, evolución temporal y variabilidad espacial*, Publicaciones del Consejo de Protección de la Naturaleza de Aragón, 2005.
- Vicente-Serrano, S. M., Lanjeri, S., and López-Moreno, J. I.: Comparison of different procedures to map reference evapotranspiration using geographical information systems and regression-based techniques, *Int. J. Climatol.*, 27, 1103–1118, 2007.
- Vogt, J. V., Viau, A. A., and Paquet, F.: Mapping regional air temperature fields using satellite

## Mapping rainfall erosivity at a regional scale

M. Angulo-Martínez et al.

Title Page

Abstract

Introduction

Conclusions

References

Tables

Figures

◀

▶

◀

▶

Back

Close

Full Screen / Esc

Printer-friendly Version

Interactive Discussion



- derived surface skin temperatures, *Int. J. Climatol.*, 17, 1559–1579, 1997.
- Weisse, A. K. and Bois, P.: A comparison of methods for mapping statistical characteristics of heavy rainfall in the French Alps: The use of daily information, *Hydrol. Sci. J.*, 47, 739–752, 2002.
- 5 Weiss, S. M. and Kulikowski, C. A.: *Computer Systems That Learn*, Morgan Kaufmann, USA, 1991.
- Willmott, C. J. and Matsuura, K.: Advantages of the mean absolute error (MAE) over the root mean square error (RMSE) in assessing average model performance, *Climate Res.*, 30, 79–82, 2005.
- 10 Willmott, C. J.: On the validation of models, *Phys. Geogr.*, 2, 184–194, 1981.
- Winchell, M. F., Jackson, S. H., Wadley, A. M., and Srinivasan, R.: Extension and validation of a geographic information system-based method for calculating the Revised Universal Soil Loss Equation length-slope factor for erosion risk assessments in large watersheds, *J. Soil Water Conserv.*, 63, 105–111, 2008.
- 15 Wischmeier, W. H.: A rainfall erosion index for a universal soil-loss equation, *Soil Sci. Soc. Am. Pro.*, 23, 246–249, 1959.
- Wischmeier, W. H. and Smith, D. D.: *Predicting rainfall erosion losses: a guide to conservation planning*. USDA Handbook 537, Washington, DC., 1978.

## HESSD

6, 417–453, 2009

### Mapping rainfall erosivity at a regional scale

M. Angulo-Martínez et al.

Title Page

Abstract

Introduction

Conclusions

References

Tables

Figures

◀

▶

◀

▶

Back

Close

Full Screen / Esc

Printer-friendly Version

Interactive Discussion



## Mapping rainfall erosivity at a regional scale

M. Angulo-Martínez et al.

**Table 1.** Regression model variables (explaining the process for each index).

Independent candidate variables		Independent variables selected for the regression model	
		<i>R</i> average (1997–2006)	<i>EI</i> <sub>30</sub> average per event (1997–2006)
LON	Longitude (m)		X
LAT	Latitude (m)		X
MED	Distance to Mediterranean Sea (m)	X	X
CANTAB	Distance to Cantabrian Sea (m)	X	
RAD	Incoming solar radiation ( $\text{J d}^{-1}$ )		X
RADx	Incoming solar radiation within $x_j$ , where $x$ is a radius of 2.5, 5 and 10 km		
ELEV	Elevation (m)		
ELEVx	Elevation within $x_j$ , where $x$ is a radius of 2.5, 5 and 10 km	X	

Title Page

Abstract

Introduction

Conclusions

References

Tables

Figures

◀

▶

◀

▶

Back

Close

Full Screen / Esc

Printer-friendly Version

Interactive Discussion



## Mapping rainfall erosivity at a regional scale

M. Angulo-Martínez et al.

Title Page

Abstract

Introduction

Conclusions

References

Tables

Figures

◀

▶

◀

▶

Back

Close

Full Screen / Esc

Printer-friendly Version

Interactive Discussion



**Table 2.** Computation of several goodness of fit statistics used on this study.

Statistical criteria	Definitions:
	$N$ : $n^o$ of observations $O$ : observed value $\bar{O}$ : mean of obs. values $P$ : predicted value $P'_i = P_i - \bar{O}$ $O'_i = O_i - \bar{O}$
Least-squares linear regression	Slope Intercept $r^2$ =coefficient of determination
Mean bias error (MBE)	$MBE = N^{-1} \sum_{i=1}^N (P_i - O_i)$
Mean absolute error (MAE)	$MAE = N^{-1} \sum_{i=1}^N  P_i - O_i $
Willmontt's $D$	$D = 1 - \frac{\sum_{i=1}^N (P_i - O_i)^2}{\sum_{i=1}^N ( P'_i  +  O'_i )^2}$

## Mapping rainfall erosivity at a regional scale

M. Angulo-Martínez et al.

**Table 3.** Coeficients regression models and predict variables selected ( $EI_{30}$  and  $R$ ).

	$r$	$r^2$	Variables
$R$ Factor	0.504	0.3406	MED,CANTAB, ELEV_10
$EI_{30}$ Index	0.528	0.2933	LON, LAT, MED, RAD

Title Page

Abstract

Introduction

Conclusions

References

Tables

Figures

◀

▶

◀

▶

Back

Close

Full Screen / Esc

Printer-friendly Version

Interactive Discussion



**Mapping rainfall erosivity at a regional scale**

M. Angulo-Martínez et al.

**Table 4.** Standardized coefficient of the regression model variables.

Variables	Standardized Coefficient
<i>R</i> Factor	
ELEV_10	0.3591
CANTAB	−1.2172
MED	−1.395
<i>E</i> / <sub>30</sub> Index	
MED	−2.563
LON	−1.622
LAT	1.034
RAD	−0.172

Title Page

Abstract

Introduction

Conclusions

References

Tables

Figures

◀

▶

◀

▶

Back

Close

Full Screen / Esc

Printer-friendly Version

Interactive Discussion



## Mapping rainfall erosivity at a regional scale

M. Angulo-Martínez et al.

**Table 5.** Accuracy measurements for factor  $R$  models: mean and standard deviation of the observed and predicted values, and cross-validations statistics.

Validation statistics	Mean	Standard deviation	$R^2$	Slope	Intercept	MBE	MAE	Willmott's $D$
Observed	891.40	621.77						
Predicted								
Inverse Distance Weighting ( $r=1$ )	896.64	292.49	0.18	0.89	720.63	5.24	355.26	0.53
Inverse Distance Weighting ( $r=2$ )	891.75	346.59	0.18	0.77	678.51	0.35	356.33	0.58
Inverse Distance Weighting ( $r=3$ )	896.85	420.40	0.17	0.60	651.23	5.44	367.40	0.59
Smoothed splines [ $T(x, y)=400$ ]	895.86	275.70	0.18	0.95	729.56	4.45	354.99	0.52
Splines with tension ( $\varphi=400$ )	896.74	268.30	0.16	0.92	744.38	5.33	357.45	0.50
Splines with tension ( $\varphi=5000$ )	890.21	324.54	0.20	0.85	684.19	-1.19	348.27	0.57
Simple kriging	901.06	274.77	0.19	1.18	758.61	9.66	362.25	0.49
Ordinary kriging	882.00	228.44	0.19	0.99	710.16	-9.40	347.83	0.54
Ordinary kriging with anisotropy	891.31	287.85	0.22	1.01	699.25	-0.09	349.18	0.56
Co-kriging	882.06	277.70	0.19	0.98	707.75	-9.34	347.77	0.54
Regression	809.94	268.26	0.15	0.89	662.28	-81.46	352.15	0.50
Regression model+residuals (inverse distance, $r=2$ )	890.77	381.76	0.19	0.71	652.96	-0.63	356.61	0.59
Regression model+residuals (spline with tension, $\varphi=400$ )	889.87	331.54	0.17	0.78	692.95	-1.53	360.34	0.55
Regression model+residuals (ordinary kriging)	881.08	323.62	0.17	0.79	689.13	-10.32	359.6	0.55

Title Page

Abstract Introduction

Conclusions References

Tables Figures

◀ ▶

◀ ▶

Back Close

Full Screen / Esc

Printer-friendly Version

Interactive Discussion



Mapping rainfall erosivity at a regional scale

M. Angulo-Martínez et al.

**Table 6.** Accuracy measurements for index  $EI_{30}$  models: mean and standard deviation of the observed and predicted values, and cross-validations statistics.

Validation statistics Model	Mean	Standard deviation	$R^2$	Slope	Intercept	MBE	MAE	Willmott's $D$
Observed	44.32	25.85						
Predicted								
Inverse Distance Weighting ( $r=1$ )	44.23	12.17	0.21	0.97	34.68	-0.10	14.60	0.56
Inverse Distance Weighting ( $r=2$ )	43.69	13.40	0.21	0.87	33.27	-0.64	14.62	0.58
Inverse Distance Weighting ( $r=3$ )	43.82	16.22	0.17	0.65	32.41	-0.50	15.17	0.58
Smoothed splines [ $T(x, y)=400$ ]	44.44	12.05	0.22	1.00	34.80	0.12	14.58	0.57
Splines with tension ( $\varphi=400$ )	44.48	11.68	0.21	1.01	35.33	0.16	14.62	0.55
Splines with tension ( $\varphi=5000$ )	44.11	13.40	0.23	0.93	33.01	-0.21	14.28	0.60
Simple kriging	44.47	12.05	0.19	1.30	37.86	0.15	15.20	0.47
Ordinary kriging	44.02	8.75	0.22	1.00	34.39	-0.30	14.64	0.57
Ordinary kriging with anisotropy	44.34	13.07	0.23	0.95	33.52	0.02	14.28	0.60
Co-kriging	44.09	12.66	0.22	0.96	33.91	-0.23	14.52	0.58
Regression	40.86	9.54	0.23	1.30	33.02	-3.46	13.73	0.50
Regression model+residuals	43.95	14.47	0.22	0.85	32.20	-0.37	14.60	0.61
(inverse distance, $r=2$ )								
Regression model+residuals	44.32	13.39	0.24	0.94	33.15	-0.001	14.65	0.60
(spline with tension, $\varphi=400$ )								
Regression model+residuals	44.26	13.42	0.23	0.92	33.29	-0.06	14.91	0.60
(Ordinary kriging)								

Title Page

Abstract Introduction

Conclusions References

Tables Figures

◀ ▶

◀ ▶

Back Close

Full Screen / Esc

Printer-friendly Version

Interactive Discussion



## Mapping rainfall erosivity at a regional scale

M. Angulo-Martínez et al.

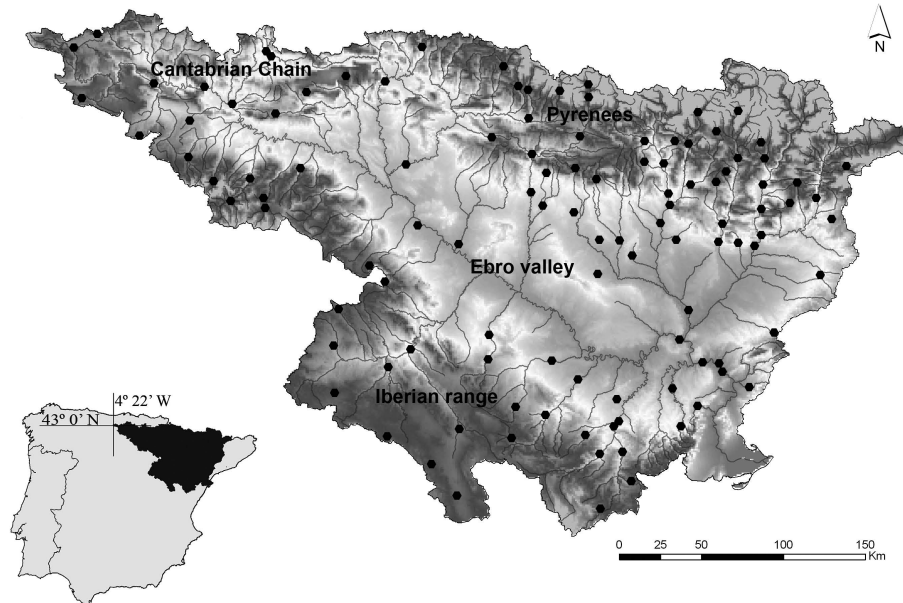


**Fig. 1.** Location of the study area and the observatories used on this study.

Title Page

Abstract

Introduction

Conclusions

References

Tables

Figures

◀

▶

◀

▶

Back

Close

Full Screen / Esc

Printer-friendly Version

Interactive Discussion



Mapping rainfall erosivity at a regional scale

M. Angulo-Martínez et al.

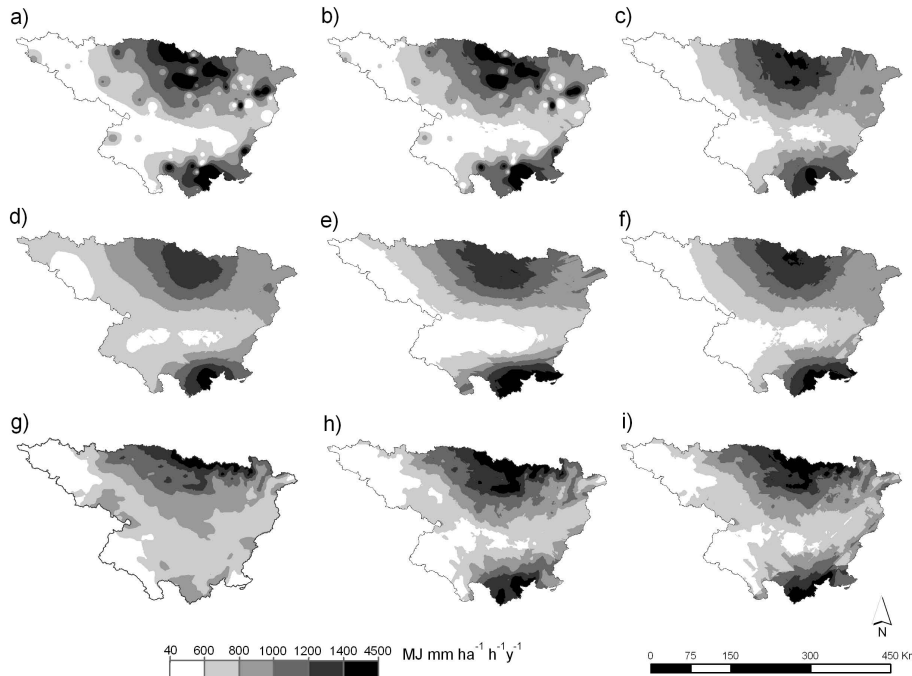


**Fig. 2.** Rainfall erosivity maps (RUSLE *R* factor) for the Ebro Basin: **(a)** Inverse Distance Weighting surface; **(b)** Spline with tension ( $\varphi=5000$ ); **(c)** Smoothing spline ( $\varphi=400$ ); **(d)** Simple kriging; **(e)** Ordinary kriging with anisotropy; **(f)** Co-Kriging; **(g)** Regression model; **(h)** Regression model+residuals interpolated by Spline with tension ( $\varphi=400$ ); **(i)** Regression model+residuals interpolated by ordinary kriging.

Title Page

Abstract

Introduction

Conclusions

References

Tables

Figures

◀

▶

◀

▶

Back

Close

Full Screen / Esc

Printer-friendly Version

Interactive Discussion



Mapping rainfall erosivity at a regional scale

M. Angulo-Martínez et al.

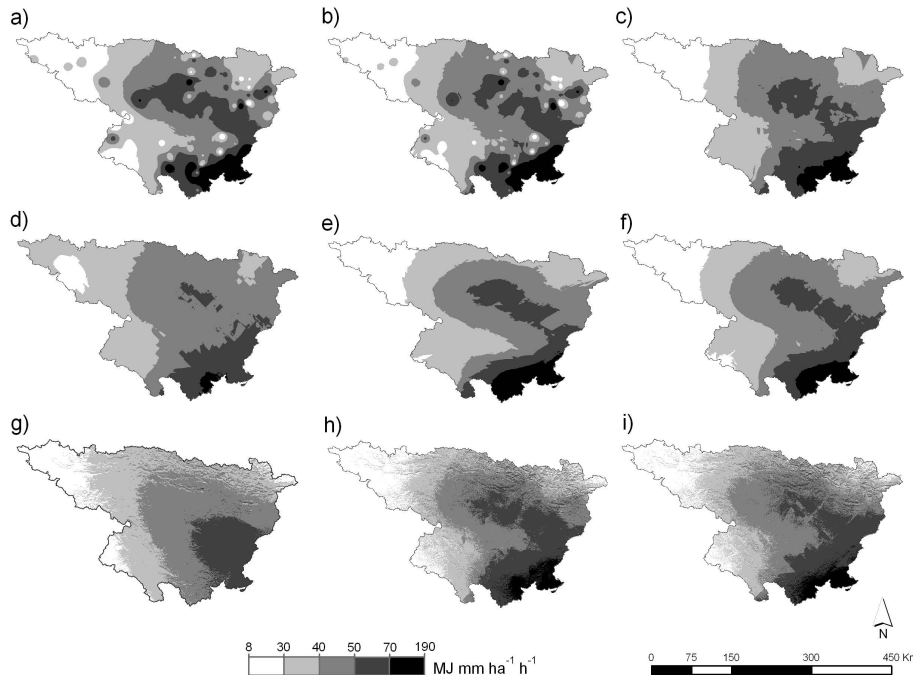


**Fig. 3.** Rainfall erosivity maps (average  $EI_{30}$  index of the erosive events) for the Ebro Basin: **(a)** Inverse Distance Weighting surface; **(b)** Spline with tension ( $\varphi=5000$ ); **(c)** Smoothing spline ( $\varphi=400$ ); **(d)** Simple kriging; **(e)** Ordinary kriging with anisotropy; **(f)** Co-Kriging; **(g)** Regression model; **(h)** Regression model+residuals interpolated by Spline with tension ( $\varphi=400$ ); **(i)** Regression model+residuals interpolated by ordinary kriging.

Title Page

Abstract

Introduction

Conclusions

References

Tables

Figures

◀

▶

◀

▶

Back

Close

Full Screen / Esc

Printer-friendly Version

Interactive Discussion



## Mapping rainfall erosivity at a regional scale

M. Angulo-Martínez et al.

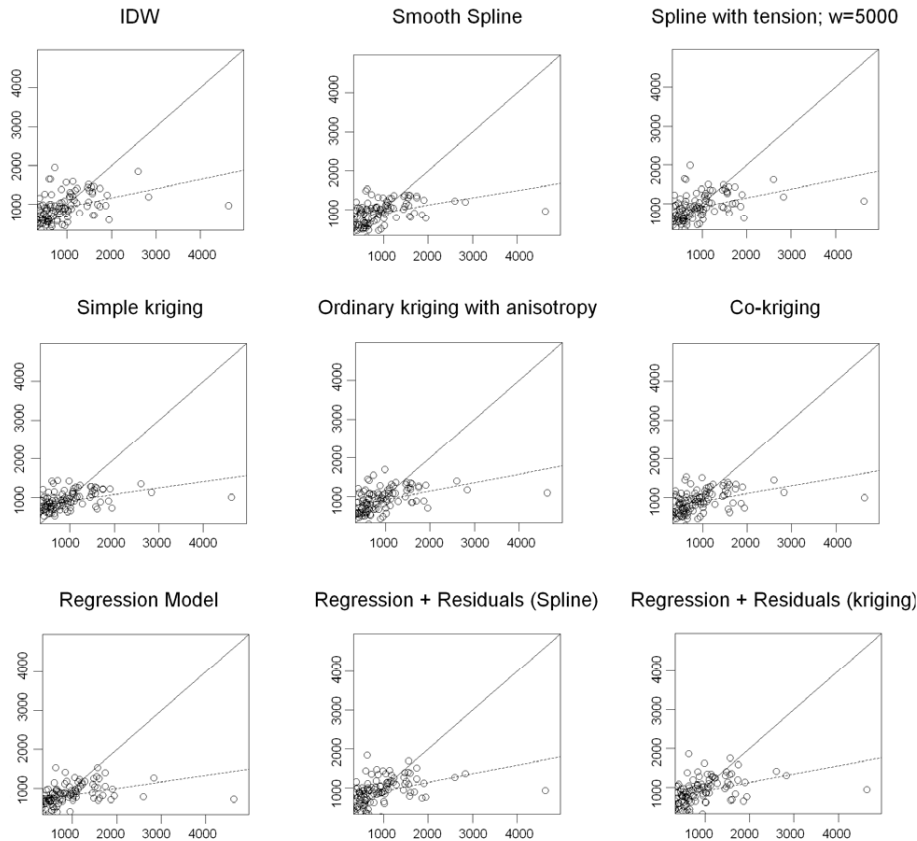


**Fig. 4.** Goodness of fit plots for the  $R$  factor: predicted vs. observed values, perfect fit line and regression line (dashed).

Title Page

Abstract

Introduction

Conclusions

References

Tables

Figures

◀

▶

◀

▶

Back

Close

Full Screen / Esc

Printer-friendly Version

Interactive Discussion



## Mapping rainfall erosivity at a regional scale

M. Angulo-Martínez et al.

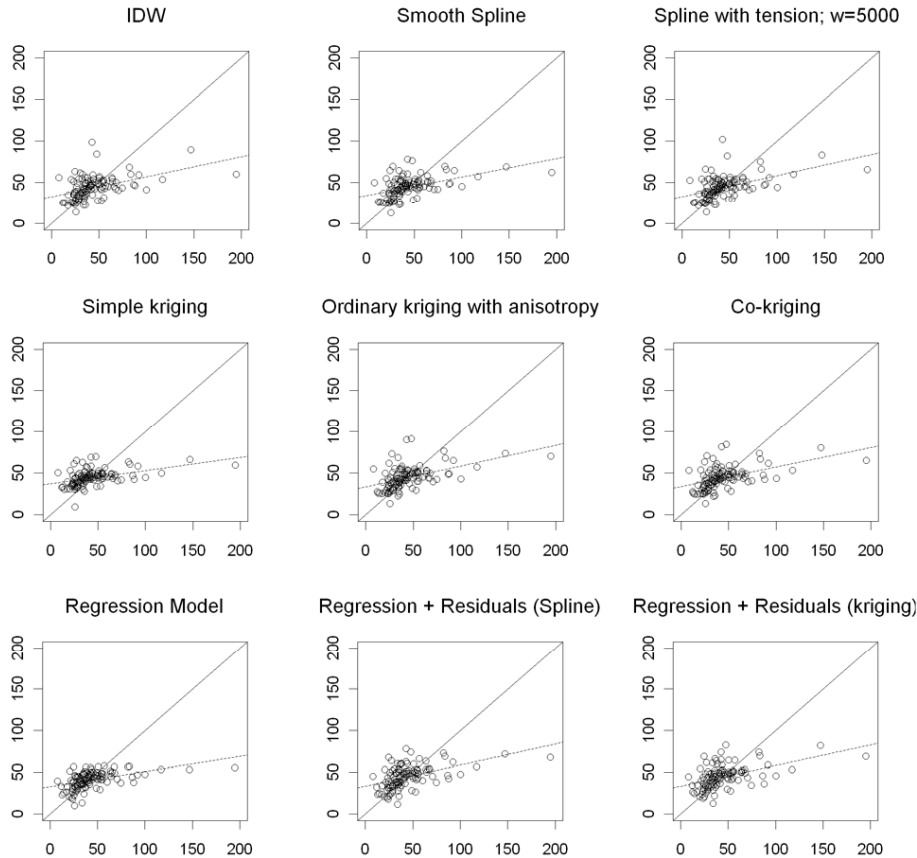


**Fig. 5.** Goodness of fit plots for the  $E/_{30}$  factor: predicted vs. observed values, perfect fit line and regression line (dashed).

Title Page

Abstract

Introduction

Conclusions

References

Tables

Figures

◀

▶

◀

▶

Back

Close

Full Screen / Esc

Printer-friendly Version

Interactive Discussion

